https://doi.org/10.5194/wes-2024-96
Preprint. Discussion started: 12 August 2024

eawe european academy of wind energy
Open Access WIND ENERGY SCIENCE DISCUSSIONS

Enabling Efficient Sizing of Hybrid Power Plants: A Surrogate-Based Approach to Energy Management System Modeling

Charbel Assaad[1], Juan Pablo Murcia Leon[1], Julian Quick[1], Tuhfe Göçmen[1], Sami Ghazouani[2], and Kaushik Das[1]

[1]Department of Wind and Energy Systems, Technical University of Denmark, Roskilde, Denmark
[2]TotalEnergies, Paris, La Défense, France

Correspondence: Charbel Assaad (chass@dtu.dk)

Abstract.

Sizing of Hybrid Power Plants (HPPs), which include wind power plants and battery energy systems, is essential to capture trade offs among various technology mixes. To accurately represent these trade-offs, an Energy Management System (EMS) is introduced to model the operation of a battery when participating in any market, resulting in realistic operational revenues and costs. However, traditional EMS models are computationally expensive to solve, a challenge that intensifies when integrating these models into sizing processes. This research paper aims to address the critical need for a computationally efficient, accurate, and comprehensive operational model that enables quantitative assessment of HPPs. A novel methodology is introduced to approximate a state-of-the-art EMS model for HPPs involved in spot market power bidding. This approach utilizes singular value decomposition for dimension reduction and a feed-forward neural network as a regression. The accuracy of our methodology is evaluated showing a root mean square error of 0.09 in predicting hourly operational time series. This method proves effective in accurately evaluating the operation of HPPs across various geographical locations and hence on multiple sizing problems. Furthermore, we utilized the surrogate to evaluate the profitability of several HPPs sizing, achieving a root mean square error of 0.010 on the profitability index. This shows that the developed surrogate is suitable for HPP sizing for given cost and financial assumptions.

1 Introduction

As the renewable energy and storage industry has matured, governmental incentives, that sustained this rapid development, started to shift. Initially sustained by government-supported feed-in tariffs, wind power plant are transitioning to feed-in premiums or contracts for differences. These support levels are now determined through competitive bidding procedures, Busch et al. (2023). Additionally, the power plants are also expected to maximize their values from energy markets such as electricity spot market or balancing/reserve markets.This change exposes power plant developers to the dynamics of the wholesale electricity market. In this evolving landscape, Battery Energy Storage Systems (BESS) are becoming valuable for wind power plants to establish robust business cases.

https://doi.org/10.5194/wes-2024-96
Preprint. Discussion started: 12 August 2024

eawe european academy of wind energy
Open Access WIND ENERGY SCIENCE DISCUSSIONS

Despite the absence of a universal definition for Hybrid Power Plants (HPPs) - highlighted by varying interpretations in the literature Dykes et al. (2020); Long et al. (2022); Paska et al. (2009) - for the purposes of this research, we define renewable-based HPPs as power plants that combine several technologies, including wind turbines, and possibly energy storage, to produce electricity and other energy vectors. They operate from a single geographical location, with all generated power being transmitted to the electrical grid via a unified point of grid connection.

In the presence of a BESS, HPPs can use strategies such as market arbitrage which involves buying and storing electricity when market prices are low and selling it when prices are high. Additionally, the integration of energy storage is crucial for smoothing power supply fluctuations, mitigating power curtailment, enabling HPPs to offer system services and reduce grid congestion Das et al. (2019).

As HPPs transition to market-driven revenue models, new possibilities and challenges emerge for power plant developers and operators. They can strategically navigate energy markets, tailor their operations to demand fluctuations, and capitalize on price differentials. Consequently, to optimally size an HPP and exploit its potential, it is crucial to consider detailed operational strategies throughout the power plant's lifetime. This role is fulfilled by an Energy Management System (EMS). A comprehensive EMS takes into account the market structure in which the power plant operates, models the various technologies within the HPP, and aims to maximize profits through market biddings. The importance of a realistic EMS becomes more apparent when a HPP includes a storage system, as it is necessary to optimize the charge and discharge power of the battery given the available resources (i.e., wind speed, solar power), the battery's capacity, available grid connection capacity and degradation cost. Electricity markets often require power producers to bid in advance for the quantity of electricity they will generate and sell. These biddings are based on forecasting of renewable energy generations as well as market prices. However, when the actual generation deviates from scheduled bids, financial penalties are incurred, accurate forecasting can mitigate these penalties. Hence, EMS operates to maximize profits, taking into account opportunities in storing and selling electricity, as well as minimizing imbalance costs due to deviations from the scheduled energy bid. Consequently, numerous studies have approached EMS modeling as an optimization problem. For instance, Das et al. (2020) established a problem formulation for a wind-battery power plant based on the day-ahead market, including regulatory periods of the Danish market structure. To account for the uncertain nature of wind speed and market prices, Crespo-Vazquez et al. (2018) formulated a two-stage convex stochastic programming framework that incorporates stochastic variables for day-ahead prices, balancing market prices, and power bidding. Several other studies have contributed to the field, formulating optimization problems under stochastic conditions (Abhinav and Pindoriya (2021); Fang and Zhao (2020)) and deterministic scenarios (Huang et al. (2021); Cai et al. (2016)). However, these formulations typically assume a given HPP configuration with fixed sizes for wind turbines and battery capacity, optimizing the system's operation within these constraints. Optimal sizing of an HPP, on the other hand, requires variations in the sizes of the wind turbines and battery energy and power, presenting a more complex challenge. Consequently, sizing an HPP based on any comprehensive and realistic EMS models involves running the EMS optimization for each potential HPP configuration, resulting in considerable computational demands. Indeed, the combination of generation and storage technologies introduce numerous time-dependent variables, complicating the optimization process for sizing an HPP. To illustrate this, we present a

https://doi.org/10.5194/wes-2024-96
Preprint. Discussion started: 12 August 2024

eawe european academy of wind energy
Open Access WIND ENERGY SCIENCE DISCUSSIONS

quantitative analysis of the required computational effort for optimal HPP sizing, based on an EMS developed by Zhu et al. (2022). This model will be further detailed in Section 2.1.

Table 1 illustrates why HPP sizing optimization often relies on a simplified EMS representation. A complex EMS can extend the optimization process to thousands of hours, making a simplified EMS a common approach to reduce computational time. Although this approach may sacrifice some accuracy in predicted operational revenues, it is a common thread in numerous review studies (Roy et al. (2022), Lian et al. (2019), Thirunavukkarasu et al. (2023)) that examine HPP sizing methodologies. These studies reveal a predominant preference for simplified operational strategies in the sizing process. The methodologies are typically divided into deterministic and stochastic mathematical-based approaches, such as linear or dynamic programming models, which are well-suited for handling differentiable and continuous objective functions. While gradient-based numerical optimization has the advantage of guaranteeing local optimality, their applicability is limited to a subset of objective functions that are continuous and convex.

To evaluate the value of HPP, the Levelized Cost of Energy (LCoE) is traditionally used. However, to assess the various potential revenue streams, metrics such as Net Present Value (NPV) Dykes et al. (2020) or the NPV over CAPEX (Capital Expenditure), are more relevant. This is because storage inherently increases costs and thus the LCoE, even though it has the potential to substantially increase revenue or profit.

Table 1. Computational Effort for Optimal Sizing of an HPP using a complex EMS from Zhu et al. (2022)

Time required for one sizing loop (sec)	10
Iteration required to find refined solution	1,000
Time required to compute EMS output per HPP configuration (sec)	2,820
Total time to find the refined configuration (sec)	28,200,000
Time in hours	**7,833**

To overcome the computational challenges associated with implementing a realistic EMS for HPP sizing while maintaining high accuracy, a promising approach involves the use of data-driven surrogate-based optimization a technique that has shown promise in addressing computationally intensive problems in other domains. For instance, Zhang et al. (2021) trained a deep reinforcement learning algorithm to derive the optimal control policy for the operation of a small-scale wind-solar-diesel-battery-reverse osmosis energy system. In a similar approach, Lin et al. (2023) developed a Kriging-based surrogate model to substitute the computationally expensive objective functions. Consequently, the combined economic and emission dispatch problem in large-scale power systems was efficiently solved with suitable accuracy. Furthermore, Pang et al. (2023) employed a neural network surrogate model to replace the original fuel cost functions, reducing the execution time. This neural network was integrated with a data-driven bat algorithm that efficiently addressed the economic dispatch problem within a comparatively shorter timeframe than other tested approaches. Despite the advancements in surrogate modeling for various applications, there remains a gap for surrogate models tailored to EMS for utility-scale HPPs incorporating detailed operational strategies

https://doi.org/10.5194/wes-2024-96
Preprint. Discussion started: 12 August 2024

eawe european academy of wind energy
Open Access WIND ENERGY SCIENCE DISCUSSIONS

for market participation. This gap exists not only due to the lack of existing applications of surrogate models for EMS in HPPs but also because of the complexity involved in designing an accurate surrogate model based on a multitude of input and output time series. Utility-scale HPPs require precise and reliable predictions to optimize performance and profitability, and the variability in market conditions and operational constraints further complicates the creation of effective surrogate models. Additionally, the surrogate model needs to be integrated within a sizing evaluation framework.

This article seeks to address the critical need for a computationally efficient, accurate, and comprehensive operational model that enables quantitative assessment of HPPs. For that, four surrogate models are used to approximate the outputs of the high-fidelity EMS. Two of which use a multivariate linear regression to establish a baseline and two others are based on Neural networks (NNs). Thanks to the variety of the NN's activation functions, the inherent non-linear behavior of the high-fidelity EMS can be approximated. This paper builds on top the EMS model developed by Zhu et al. (2022), which will be detailed in the following section.

The major contributions of this article are:

- Development of a fast and precise surrogate for a utility-scale HPP EMS model participating in the spot market. The surrogate is based on a Feed-Forward Neural Network (FNN), harnessing the power of machine learning to provide a reliable and efficient alternative to the computationally intensive EMS model.
- Assessment of the surrogate's ability to predict hourly operational time series on multiple sites across the same electricity market region.
- Integration of the developed surrogate within a framework to evaluate the profitability of an HPP sizing with high accuracy.

The remainder of this paper is organized as follows. Section 2 introduces the EMS model that the surrogate is based on, the methodology devised for the surrogate modeling of the EMS, and the sizing evaluation framework for analyzing the profitability of an HPP. Section 4 provides details on the data used to train and validate the surrogate as well as the cost model for the sizing evaluation framework. While Section 5 provides an in-depth analysis of the surrogate's accuracy and its application. These results are put into perspective in Section 6 and summarized in Section 7.

2 Methodology

In this section, we will start by presenting the high-fidelity model that serves as the foundation for the surrogate models, Section 2.1, followed by the methodology for developing the surrogate model in Section 2.2.

2.1 HPP Operation Model (EMS)

The EMS model, on which the surrogate is built, is presented in this section. The EMS model is based on a study by Zhu et al. (2022) that focused on a co-located wind-battery HPP. This novel EMS model, was formulated to optimize market participation

https://doi.org/10.5194/wes-2024-96
Preprint. Discussion started: 12 August 2024

eawe european academy of wind energy
Open Access WIND ENERGY SCIENCE DISCUSSIONS

within two sequential electricity markets: namely, the spot market (SM) and the Balancing Market (BM), which encompasses the regulatory periods of the Danish market structure. This state of the art EMS has the advantage of considering:

- Long-term operation of the HPP with comprehensive revenue streams calculations.
- Grid capacity, as a practical constraint for the HPP.
- Possibility of considering overplanting, which has been shown to increase the value of HPP.

In electricity trading, various markets enable power plant operators to sell their energy. The SM is currently the most lucrative market where power is traded for immediate delivery. In the SM, power plant operators can bid on the day-ahead and hour-ahead markets. Day-ahead bidding determines hourly prices for the next day, while hour-ahead biddings allows for adjustments based on updated generation forecasts and cleared SM prices. The BM, another potential source of revenues for HPPs, operates in conjunction with the Spot Market (SM). The BM enables transmission system operators to adjust for discrepancies between forecasted and actual demand and supply. These discrepancies arise from the predicted electricity supply that were forecasted during the SM bidding process and the actual conditions closer to the delivery time. Hence, the BM acts in near real-time, penalizing deviations from scheduled generation. This paper primarily focuses on the EMS's role in Day-Ahead (DA) SM participation. Additionally, our study considers the Danish market structure with a dispatch interval of 15 minutes. As in real power plants, the EMS communicates with a Power Management System (PMS). In this framework, the EMS provides energy set-points, based on weather and market forecast data to the PMS, which, in turn uses Real-Time (RT) measurement data to derive RT power values. RT measurements allow the calculation of deviations and the applications of penalties. The PMS is emulated as an active power control logic, as described in Long et al. (2022). The inputs to the EMS are time series forecasts of wind power and market prices, while the PMS use the same input time series updated to RT measurements, for each dispatch interval, as well as the bidding schedule generated from the EMS. For clarity, inputs and outputs of the EMS and PMS are listed in Table 2.

Table 2. Inputs and Outputs of EMS and PMS from Zhu et al. (2022). RT stands for Real-Time.

Model	Inputs	Outputs
EMS	HPP configuration	HPP power output schedule
	Wind power forecast	Battery charge/discharge power
	SM price forecast	Battery state of charge
PMS	Same as EMS, and	RT HPP power output
	RT wind power	RT battery charge/discharge power
	Cleared SM prices	RT battery state of charge
	EMS power output schedule	RT curtailed power

While the EMS's inputs and output time series are based on hourly time steps, the PMS's outputs and RT input time series have a time step equal to the dispatch interval i.e., 5 min for the the Danish market structure. Additionally, both models

https://doi.org/10.5194/wes-2024-96
Preprint. Discussion started: 12 August 2024

eawe european academy of wind energy
Open Access WIND ENERGY SCIENCE DISCUSSIONS

assume a given HPP configuration, also denoted as sizing parameters in this article. They are defined as the wind power plant rated power, the rated battery power rating, battery energy capacity rating, and grid connection power capacity. Other battery parameters such as the charge/discharge efficiency are assumed from Zhu et al. (2022).

Figure 1 illustrates the considered EMS workflow.

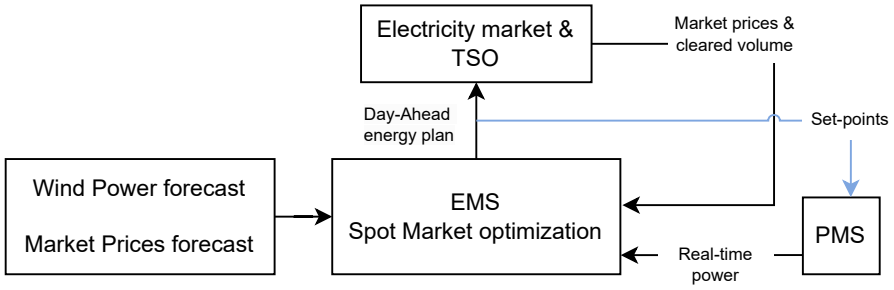

Figure 1. EMS for Spot Market workflow. Adapted from Zhu et al. (2022)

The EMS itself is formulated as a Mixed Integer Linear Programming (MILP) model, executed once daily, at the beginning of each day. It aims at maximizing the revenues throughout the time span of the inputs. The PMS takes the form of a Mixed Integer Quadratic Programming (MIQP) model, executed at regular dispatch intervals. The PMS minimizes the difference between the power bidding on the SM and the real-time available power. The details of both models can be found in the referenced work.

The optimization models were solved using the solver of IBM Decision Optimisation Studio CPLEX through the docplex python library (IBM, 2023) operating on the DTU's high-performance computing cluster Sophia Technical University of Denmark (2019).

It was observed that for a given HPP configuration, 47 minutes were required to compute the outputs for one year of operation. The underlying reason for this is due to the iterative and sequential nature of the framework. For each day, the MILP optimization is solved first followed by the MIQP for each dispatch interval (e.g. 96 times a day). While each iteration of the MILP and MIQP problems requires a minimal amount of time (less than 0.15 seconds), the frequency of these optimizations is substantial. Moreover, since each time step depends on the previous one, it is necessary to perform the optimization sequentially. Table 3 shows the number of decision variables and constraints required to optimize for inputs spanning over one year. This highlights the substantial computational time that would be required to optimize the sizing of a HPP based on such an operational model.

While the combination of both models allows for a realistic representation of the operation of a HPP, it has its own limitations. These limitations are also carried over to the surrogate that is build upon both models. No battery degradation model is considered in the optimization process. It is well known that lithium-ion batteries' energy capacity degrade over time in a non-linear fashion (Xu et al. (2018)), this directly impacts revenues as opportunities for energy arbitrage are reduced. Additionally, as we are focusing on demonstrating the potential of surrogate modeling for EMS of HPP, perfect forecast data will be used.

https://doi.org/10.5194/wes-2024-96
Preprint. Discussion started: 12 August 2024

eawe european academy of wind energy
Open Access WIND ENERGY SCIENCE DISCUSSIONS

Table 3. Annual Computational Complexity of EMS and PMS

Model	Design variables	Constraints
EMS	289,445	350,765
PMS	315,360	420,480

Finally, the balancing market will not be considered in this article and will be left as a future works. The combined models, EMS and PMS, are referred to as a high-fidelity EMS model in this paper.

2.2 Surrogate Methodology

In this article, a surrogate model consists of several sub-components: data pre-processing, a regressor, and data post-processing. The pre-processing consists of scaling that ensures all inputs contribute equally to the model's predictions and helps the surrogate's convergence algorithm. The post-processing is applied in accordance with the pre-processing to interpret the results in their original scale. The regressor is the model tasked with approximating the high-fidelity EMS. Section 2.2.1 details the inputs and outputs for training and evaluating the surrogate models. Section 2.2.2 describes four surrogate models, differing in their data processing and regressor model. Sections 2.2.3 and 2.2.4 cover the training and validation of these models, respectively.

2.2.1 Surrogate Model's Inputs and Outputs

Regardless of the surrogate model being evaluated, all models aim to approximate the same output time series given the same input data. Table 4 below lists the various input and output time series used to train and validate the surrogate.

Table 4. Input and output time series of surrogate models

	Variable	Time step	Time horizon
Input	SM price forecast: SM_t Wind power forecast: W_t	15 min	1 day
Output	HPP power output: P_t^{sm} Battery discharging power: $P_t^{sm,dis}$ Battery charging power: $P_t^{sm,cha}$ HPP curtailed power: $P_t^{sm,curt}$	1 hour	1 day

https://doi.org/10.5194/wes-2024-96
Preprint. Discussion started: 12 August 2024

eawe european academy of wind energy
Open Access WIND ENERGY SCIENCE DISCUSSIONS

The input time series of the surrogate match those of the EMS, and its outputs align with the PMS's outputs. In addition to the input time series, the regressor also considers three scalar parameters representing an HPP, which helps differentiate between various HPP configurations. They are represented by equations 1 to 3:

$$P^W/P^G \tag{1}$$

$$B^P/P^G \tag{2}$$

$$B^E/B^P \tag{3}$$

Where P^W is the rated power of the wind power plant, P^G is the grid connection capacity, B^P is the rated battery power, and B^E is the rated energy capacity of the battery.

2.2.2 Surrogate Models

Table 5 presents all surrogate models evaluated.

Table 5. Surrogate models tested

Pre-processing	Regressor	Post-processing
Normalization	Linear	Reverse Normalization
Normalization SVD	Linear	Reverse SVD Reverse Normalization
Normalization	FNN	Reverse Normalization
Normalization SVD	FFN	Reverse SVD Reverse Normalization

The first surrogate, which serves as our benchmark, normalizes the input and output time series for each HPP configuration and employs a multivariate linear regression to predict the normalized outputs from normalized inputs. Details on the normalization process appear later on, in this section.

The second surrogate incorporates a dimensionality reduction method known as Singular Value Decomposition (SVD), as developed by Gene H. Golub (1996). After normalizing inputs and outputs, we apply SVD, a common tool in numerical analysis, particularly for dimensionality reduction. The specific use of this method is detailed in this section.

The third and fourth surrogate models are similar to the first and second ones, but they differ in their choice of regressors. Instead of employing a multivariate linear model, these models utilize a tuned FNN to capture the non-linear relationships between inputs and outputs. For all surrogate models, we apply data post-processing consistent with the pre-processing to ensure the output data is interpretable in its original scale.

https://doi.org/10.5194/wes-2024-96
Preprint. Discussion started: 12 August 2024

eawe european academy of wind energy
Open Access WIND ENERGY SCIENCE DISCUSSIONS

For all surrogate models, we normalize the wind power generation time series (W_t) using the turbine's rated power, and the spot market price time series (SM_t) by the maximum price, achieving a scaling between zero and one. Since the output time series magnitudes depend on the sizing inputs, we use these parameters as the basis for normalization. This step refers to the Normalization in Table 5. It is applied for each time series following these equations:

$$P^{sm}_{t,norm} = P^{sm}_t / P^G \tag{4}$$

$$P^{sm,dis}_{t,norm} = P^{sm,dis}_t / B^P \tag{5}$$

$$P^{sm,cha}_{t,norm} = P^{sm,cha}_t / B^P \tag{6}$$

$$P^{sm,curt}_{t,norm} = P^{sm,curt}_t / (P^W - P^G) \tag{7}$$

In Equation (4) the power bidding on the SM is normalized by the grid capacity. Equations (5) and (6) normalized the battery charge and discharge profiles by the battery's rated capacity, and Equation (7) normalized the curtailed power with respect to the difference between wind power and grid capacity. A surrogate model, using only normalization for data processing, has five input features: SM_t, W_t, P^W/P^G, B^P/P^G, and B^E/B^P. It outputs four features: P^{sm}_t, $P^{sm,dis}_t$, $P^{sm,cha}_t$, and $P^{sm,curt}_t$.

We apply SVD method, as described in Zhu et al. (2010), to derive the principal component matrices, denoted as Z in the cited paper. This method is used independently for the matrices containing the input time series M_{in} and the output time series M_{out}. The SVD is used following the normalization described above and it is applied for the 2^{nd} and 4^{th} surrogate models of Table 5. Figure 2 illustrates the matrix M_{in}, which includes all input time series for a single HPP configuration.

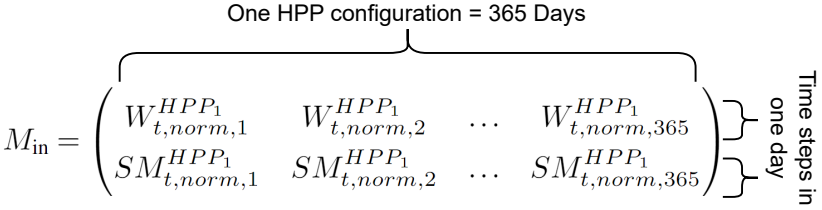

Figure 2. Matrix M containing input time series, denoted M_{in}

In this figure, the notation $W^{HPP_n}_{t,norm,d}$ refers to the normalized wind power time series for day *d* and for the HPP configuration *n*. Similarly, $SM^{HPP_n}_{t,norm,d}$ refers to the normalized SM prices for day *d* for the HPP configuration *n*. As the high-fidelity EMS uses hourly time steps for forecasted wind power and SM prices, each of the input vector, $SM^{HPP_n}_{t,norm,d}$ and $W^{HPP_n}_{t,norm,d}$, is of shape $(24, 1)$. Hence, for a given HPP configuration, matrix M_{in} from Figure 2 is of shape $(24 \cdot 2, 365)$. To expand this matrix for all HPP configurations, we concatenate horizontally (i.e, along the second dimension) each matrix M_{in} corresponding to a HPP configuration. We thus obtain a matrix of shape $((24 \cdot 2) \cdot N, 365)$. Where N is the number of HPP configurations.

https://doi.org/10.5194/wes-2024-96
Preprint. Discussion started: 12 August 2024

eawe european academy of wind energy
Open Access WIND ENERGY SCIENCE DISCUSSIONS

The output time series matrix M_{out}, is constructed in a similar fashion. However, unlike M_{in}, this matrix contains fours time series, the ones defined in equation (4) to (7). Additionally, these time series have a time step equal to the dispatch interval e.g., 15 min. Thus, M_{out} will be of shape $((96 \cdot 4) \cdot N, 365)$.

After applying Singular Value Decomposition (SVD) to both matrices, M_{in} and M_{out} , we extract their principal component matrices, Z_{in} and Z_{out}, and truncate them to the desired level. As a result, we obtain two sets of matrices with different truncation levels, denoted as r_{in} and r_{out} respectively. We use these truncated matrices for training and evaluating the regressor models.

Table 6 presents an overview of the features and samples of each data-processing method for input and output data spanning over a year.

Table 6. Features and Samples of Data-processing methods

Data processing		**Normalization**	**SVD**
Inputs	Features	5	$r_{in} + 3$
	Samples	$(24 \cdot 2) \cdot 365 \cdot N$	$365 \cdot N$
Outputs	Features	4	r_{out}
	Samples	$(96 \cdot 4) \cdot 365 \cdot N$	$365 \cdot N$

From this table, we observe that the features of the SVD method are most likely higher than than the one derived from the normalization method (this depends on the truncation level). However, the number of samples are substantially lower, this allows us to achieve a reduced representation of the data.

2.2.3 Surrogate Training

To train a surrogate model, a training dataset is defined based on a number of HPP configurations with distinct sizing parameters. The details of this dataset can be found in Section 4. More specifically, this training dataset is used to train the SVD transformation and the two regressor models. Note that the normalization does not require a training. Two models are used to approximate the outputs of the high-fidelity EMS: a tuned FNN and a multivariate linear regression. The latter is used as a baseline model to compare the accuracy of the neural networks.

The training of FNN with hidden layers is done in two steps. Initially, a tuning process is carried out using two hyperparameters shown in Table 7 below. Afterwards, the best-performing model from the tuning process is selected for a more exhaustive training.

Within this tuning process, it's important to note that each layer can have a varying number of neurons within the provided range. A Rectified Linear Unit (ReLu) activation function has been used for all hidden layers and, for the output layer, a linear activation function has been used. ReLu is an appropriate activation function for the data, particularly following the normalization process, as all input and output time series become non-negative.

https://doi.org/10.5194/wes-2024-96
Preprint. Discussion started: 12 August 2024

eawe european academy of wind energy
Open Access WIND ENERGY SCIENCE DISCUSSIONS

Table 7. FNN grid search hyperparameter space

Hyperparameter	Range	Step
Layers	[3,9]	1
Neurons per layer	[40,80]	20

To efficiently select the hyperparameters among the search space, Hyperband by Li et al. (2018), is used. Hyperband uses random sampling of hyperparameters to explore a wide range of settings.

A NN is defined by its architecture, parameters, and hyperparameters. The architecture consists of layers, starting with the input layer whose neuron count is determined by the dimensionality of the input data. This layer is followed by several hidden layers with a given number of neurons and activation functions. These layers and neurons defines the network's depth and width, while the activation functions can introduce non-linearity into the model. The output layer has as many neurons as the variables in the output data. The interconnections between these layers defines the topology of the NN. The parameters of the NN are the learnable weights and biases, which are determined in the training process. In contrast, the hyperparameters are pre-defined settings that are not learned from the training data. These encompasses the number of hidden layers, neurons per layer and much more. To train a NN, at least 2 settings need to be defined. First, a loss function, which is a metric that measure the error between the training data and the model's prediction - the mean squared error was used. Second, an optimizer, which modifies the model's weights and biases during the training process to minimize the loss function. Each optimizer has its own set of hyperparameters. The Adam optimizer by Kingma and Ba (2017) was used with a learning rate of 10^{-4}

The tuning process aims to evaluate several thousands of NN architectures. To avoid a computationally expensive process, these NN aren't trained until they converge. Instead, the best-performing model, from the tuning process, is selected for further training.

The tuning resulted in the architectures presented in Table A1 and A2 in A

The multi-variate linear regression is trained using the same dataset with the objective of minimizing the mean squared error using the same optimizer as for the FNN.

Similarly, the SVD transformations were trained on the training dataset. The transformations were trained separately for both input and output time series, resulting in two distinct transformations. The normalization requires no training.

2.2.4 Surrogate Validation

We aim to identify the surrogate model offering the best compromise between training time, inference time, and accuracy. First, we assess each surrogate's accuracy on a validation dataset, which is separate from but defined similarly to the training dataset. We measure the accuracy of each surrogate using the Root Mean Square Error (RMSE) between the predicted and

https://doi.org/10.5194/wes-2024-96
Preprint. Discussion started: 12 August 2024

actual values for the normalized hourly time series. The RMSE is computed as follows:

$$RMSE = \sqrt{\frac{1}{N}\sum_{i=1}^{N}(y_i - \hat{y}_i)^2} \tag{8}$$

Where:

y_i is the true data, within the validation dataset

$\hat{y}_i$ is the predicted data, based on validation dataset inputs

N is the number of data points

Since this RMSE takes into account all the output time series, it provides a holistic measure of the model's accuracy. We use this metric to compare the performance of the surrogate models presented in Table 5. Additionally, we measure the training an inference time of each model.

For the best-performing surrogate model, we further investigate the accuracy of each output time series using RMSE for a deeper understanding of the model. Our focus then shifts to one specific output time series, the normalized power output $P^{sm}_{t,norm}$. This time series allows us to calculate the yearly revenues, which are required to compute the Profitability Index (PI), the key application of our surrogate in this article.

To explore the methodology's potential further, we assess the surrogate's generalizability across various locations within the western Danish price region, DK1. For this intra-generalizability analysis, we calculate the Normalized RMSE (NRMSE) of yearly revenues, defined as follows:

$$NRMSE = \frac{\sqrt{\frac{1}{K}\sum_{k=1}^{K}(\Pi_k - \hat{\Pi}_k)^2}}{Median(\Pi)} \tag{9}$$

Where:

K is the number of HPP configurations.

in the validation dataset.

Π_k is the revenue of the k^{th} HPP configuration,

based on true data.

$\hat{\Pi}_k$ is the revenue of the k^{th} HPP configuration,

based on predicted data.

Median(Π) is the median revenue of all HPP

configurations, based on true data.

https://doi.org/10.5194/wes-2024-96
Preprint. Discussion started: 12 August 2024

The revenues time series is extracted from either true/observed data (from the high-fidelity model) or predicted (from the surrogate model) power time series as follows:

$$\Pi = \sum_{i=t}^{T} P_t^{sm} \cdot \lambda_t^{sp} \cdot \Delta t \tag{10}$$

Where Π is the yearly revenue, Δt the time step, and T the total time steps within a year.

3 Application: PI Evaluation

To assess the business case of a HPP, we can use financial metrics like Internal Rate of Return (IRR) and Net Present Value (NPV). IRR calculates the HPP's annual investment return, while NPV assesses its profitability in today's value. However, when an HPP isn't profitable, resulting in a negative NPV, the IRR becomes undetermined. A more meaningful measure is the Profitability Index (PI), calculated as NPV divided by the initial investment (CAPEX). The PI indicates how many dollars of present value benefit are generated per dollar of investment, offering a more intuitive understanding of the investment's profitability. This metric allows for a direct comparison of the relative profitability of each project, regardless of their absolute size. Additionally, when resources are limited, NPV/CAPEX can aid in prioritizing projects. Projects with higher PIs can be prioritized as they promise greater returns per unit of investment. A PI greater than 1 signifies that the NPV of future cash flows exceeds the initial investment.

To compute the PI, we require the NPV which in turn requires accurate yearly revenues and costs over the HPP's lifetime, aligning with the ideal framework shown in Figure 3a. Yet, as discussed in the Introduction and Section 2.1, this method is computationally demanding. We instead use an alternative framework in Figure 3b, utilizing the developed surrogate. This surrogate replaces the high-fidelity EMS, significantly reducing computational time and making the framework's execution feasible. The accuracy of this framework, employing the surrogate model to evaluate the PI, is presented in Section 5.4.

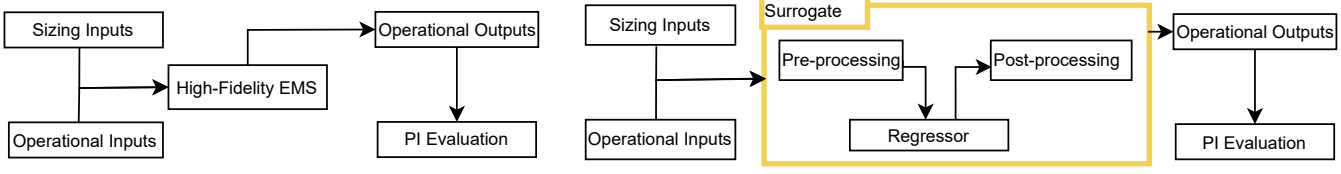

(a) Ideal sizing evaluation framework using the High-Fidelity EMS

(b) Developed sizing evaluation framework using a surrogate of the EMS

Figure 3. High-level sizing framework

The PI is calculated as follows:

$$PI = \frac{NPV(x)}{CAPEX(x)} \tag{11}$$

https://doi.org/10.5194/wes-2024-96
Preprint. Discussion started: 12 August 2024

eawe european academy of wind energy
Open Access WIND ENERGY SCIENCE DISCUSSIONS

Where:

$$x = [P^G, P^W, B^E, B^P]$$

The financial model is based on the yearly cashflow (CF_y) and the discount rate after tax (r_{AT}) as defined below:

$$NPV = \sum_{y}^{Y} \frac{CF_y}{(1+r_{AT})^y}$$

Where Y is the lifetime of the power plant. The cashflow is calculated based on yearly profits ($Profit_y$) and CAPEX .

$$CF_y = \begin{cases} Profit_y & \text{for } y > 0 \\ -CAPEX & \text{for } y = 0 \end{cases}$$

It is important to highlight that the yearly profits are based on the revenues from the surrogate or the high-fidelity EMS (Π_y), as well as, the Operational Expenditure ($OPEX_y$), the tax rate (τ_{tax}), and the r_{AT}.

$$Profit_y = (\Pi_y - OPEX_y) \cdot (1 - \tau_{tax})$$

The cost model used to calculated the $CAPEX$ and $OPEX$ is define below:

$$\begin{aligned} CAPEX &= C_w + C_b + C_{el} \\ OPEX_y &= O_{w,y} + O_{b,y} + O_{el,y} \\ C_w &= (WT_{cost} + WT_{civil}) \cdot P^W \\ C_b &= Nb_{eq} \cdot B^E_{cost} \cdot B^E + (B^P_{cost} + B^P_{civil} + B^P_{control}) \cdot B^P \\ C_{el} &= (HPP_{BOS} + P^G_{cost}) \cdot P^G + Land_rent \\ O_{w,y} &= WT^{OM}_{fixed,y} \cdot P^W + mean(AEP) \cdot WT^{OM}_{variable,y} \\ O_{b,y} &= B^{E,OM}_y \cdot B^E \\ O_{el,y} &= 0 \end{aligned}$$

Where C_w, C_b, C_{el} are the CAPEX of the wind power plant, batteries and the balance of system. Similarly $O_{w,y}$, $O_{b,y}$, and $O_{el,y}$ are the yearly OPEX from the wind power plant, batteries, and balance of system. The WT_{cost} and WT_{civil} are the wind turbine's cost and civil works in $Euro/MW$. Nb_{eq} is the number of battery equivalent in today's value. We will elaborate on this metric shortly. B^E_{cost} is the battery energy cost per MWh while B^P_{cost}, B^P_{civil}, $B^P_{control}$ are the battery power cost, civil costs and control system costs per MW. HPP_{BOS} and P^G_{cost} are the shared Balance Of System (BOS) cost and grid connection cost of the HPP. $WT^{OM}_{fixed,y}$ and $WT^{OM}_{variable,y}$ are the fixed and variable Operation and Maintenance (O&M) costs of the wind turbine per year and per MW. $mean(AEP)$ is the mean Annual Energy Production (AEP) of the wind power plant. $B^{E,OM}_y$ is the yearly O&M cost of the battery per MWh. In this study, we set a fixed lifetime for the battery (i_b) as battery degradation is not considered. Additionally, to address the decreasing costs of batteries over time, we employ the concept of equivalent

https://doi.org/10.5194/wes-2024-96
Preprint. Discussion started: 12 August 2024

eawe european academy of wind energy
Open Access WIND ENERGY SCIENCE DISCUSSIONS

number of present batteries (Nb_{eq}). This method incorporates the annual battery price reduction rate (f_b) and the designated replacement year for each battery ($yb(ib)$).

$$Nb_{eq} = \sum_{i_b=0}^{N_b-1} (1 - f_b)^{y_b(i_b)}$$

It should be noted that the calculation of NPV/CAPEX requires only the HPP power output time series from either the high fidelity model or the surrogate.

4 Case Study

In Section 4.1, we will introduce the training and validation dataset. Following this, Section 4.2 will discuss the data related to the intra-generalizability analysis. Lastly, Section 4.3 will provide a detailed overview of the cost model data specific to our application.

4.1 Training and Validation Dataset

4.1.1 HPP configurations

As we rely on a surrogate to replace the high-fidelity EMS, we require a comprehensive dataset to train and validate this surrogate. Therefore, a wide range of HPP configurations should be covered. In addition, these configurations need to be realistic and in line with industry practices. Table 8 summarize the parameter ranges.

Table 8. Sizing Parameters and Ranges

Sizing Parameter	Range
P^W/P^G [-]	[1, 2]
B^P/P^G [-]	[0, 1]
B^E/B^P [h]	[1, 8]

Where B^P is the rated battery power, P^G is the grid connection, P^W is the rated power of the wind power plant, and B^E is the energy capacity of the battery. For this article, the grid connection varies between 50 MW and 700 MW.

To ensure an equal distribution of all variables across the entire parameter space, the Latin Hypercube Sampling (LHS) method, by Jin et al. (2005), was used to randomly select 250 sizing configurations. Of which 200 HPP (80%) are used to train the regressor and 50 HPP (20%) are used to evaluate the accuracy of the surrogate as detailed in Section 2.2.2. Subsequently, the high-fidelity EMS was solved using these configurations with the input time series presented in the section below.

https://doi.org/10.5194/wes-2024-96
Preprint. Discussion started: 12 August 2024

eawe european academy of wind energy
Open Access WIND ENERGY SCIENCE DISCUSSIONS

4.1.2 Input time series & WT technology

The input time series required for the high-fidelity model, mentioned in Table 2, are generated using two tools. Wind power time series are simulated with the CorRES simulation tool Murcia Leon et al. (2021); Koivisto et al. (2019). This tool is based on re-analyzes meteorological data from the Weather Research and Forecasting model. CorRES' stochastic model, Koivisto et al. (2020b), was integrated to add fluctuations resulting in wind power time series with 15 minute-level resolution. The simulation was based on meteorological data from the year 2012, with the assumption that the climate in 2030 remains unchanged from 2012. CorRES requires specific inputs are required, including the HPP's longitude, latitude, hub height of the wind turbine, power curve, and the simulation period. The considered turbine is the Gamesa G80 with a rated power of 2MW and a hub height of 100 meters.

SM price time series for the 2030 electricity markets are obtained from the Balancing Tool Chain (BTC) Kanellas et al. (2020). BTC is built upon Balmorel, an open-source energy system modelWiese et al. (2018) that simulates electricity market operations, ranging from day-ahead to real-time dynamics for the northern central European region. Additionally, an investment optimization is implemented to simulate a 2030 energy system scenario Koivisto et al. (2020a). The wind generation and price time series are presented in the figure below:

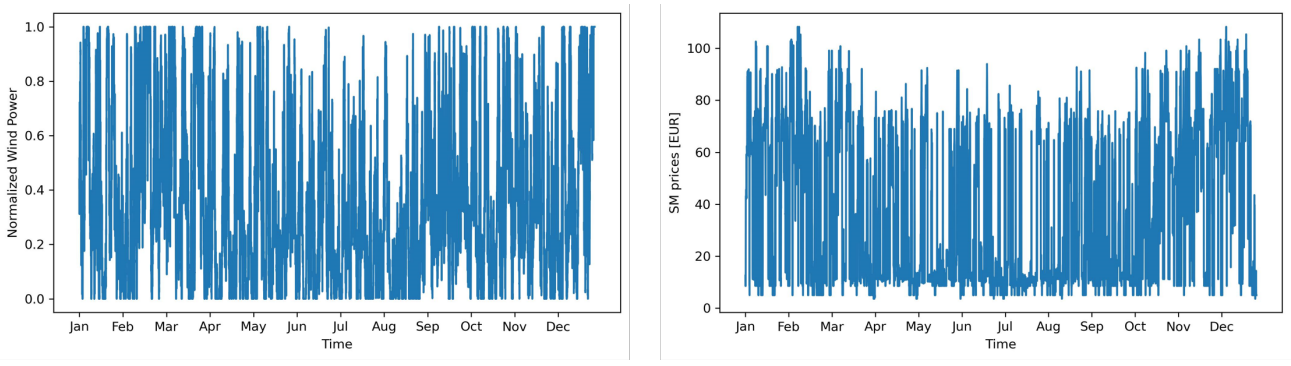

(a) Normalized wind generation (b) Normalized wind generation

Figure 4. Input time series for each HPP configuration

4.1.3 Output time series

For all 250 HPP configurations, and the above mentioned input time series, the high-fidelity model is used to generate all output time series described in the Table 4. The 200 HPP configurations, the input time series, and the output time series are used train all surrogate models.

https://doi.org/10.5194/wes-2024-96
Preprint. Discussion started: 12 August 2024

eawe european academy of wind energy
Open Access WIND ENERGY SCIENCE DISCUSSIONS

4.2 Intra-generalizability analysis Data

For the intra-generalizability analysis, we use the best surrogate model following the methodology described in Sections 2.2. We then test the surrogate's accuracy across four randomly chosen locations within the same market region, labeled A to D. At each location, we randomly select 10 HPP configurations from the training dataset and another 10 from the validation dataset. The coordinates of each location are listed in Table B1. Figure 5a displays these locations, indicating the training location with an "X" and the evaluation sites for the HPPs.

As all locations are in the same market region, the SM price time series is the same for all locations. The weather data for locations A-D were provided by CorRES and the output time series per location and per HPP configuration were generated using the high-fidelity EMS model. This data is used to compare the performance of the surrogate trained on location X and evaluated on locations A-D.

The wind generation distribution across all locations are available in Figure 5b. From this figure, it is observed that location C presents a different distribution than the other locations, notably with a lower average wind power. Meanwhile, locations A, B, and D share similar distributions.

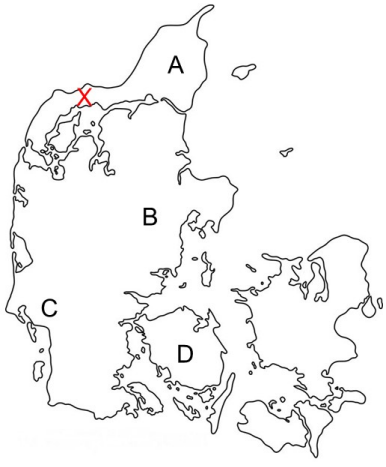

(a) Location of trained surrogate (X, in red) and evaluated model (A-D)

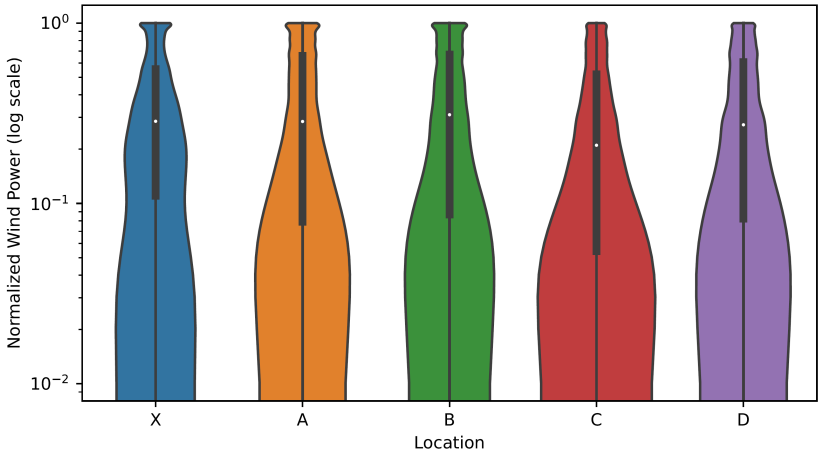

(b) Normalized wind power distribution across all locations. A log scale was used to highlight the differences between locations.

Figure 5. Intra-generalizability data

4.3 Cost model Data

Table 9 presents a summary of the cost assumptions used in this article.

As the battery's lifetime is of 7 years, each HPP will require 3 batteries during its lifetime. Given a battery price reduction of 10% per year, we obtain a number of battery equivalent (Nb_{eq}) of 1.84.

https://doi.org/10.5194/wes-2024-96
Preprint. Discussion started: 12 August 2024

eawe european academy of wind energy
Open Access WIND ENERGY SCIENCE DISCUSSIONS

Table 9. Cost assumptions

Variable	Value
r_{AT}	6%
τ_{tax}	22%
WT_{cost} [EUR/MW]	457,143
WT_{civil} [EUR/MW]	185,714
$WT^{OM}_{fixed,y}$ [EUR/MW/year]	9,000
$WT^{OM}_{variable,y}$ [EUR/MWh/year]	0.964
B^{E}_{cost} [EUR/MWh]	90,000
B^{P}_{cost} [EUR/MW]	32,000
B^{P}_{civil} [EUR/MW]	36,000
$B^{P}_{control}$ [EUR/MW]	9,000
$B^{E,OM}_{y}$ [EUR/MWh/year]	0
f_b	10%
i_b, lifetime of battery [years]	7
Y, lifetime of HPP	25
HPP_{BOS} [EUR/MW]	119,940
P^{G}_{cost} [EUR/MW]	50,000

5 Surrogate Results

This Section details the accuracy of the surrogate models and their main application in evaluating the Profitability Index (PI) of Hybrid Power Plants (HPPs). We start by comparing the accuracy of each surrogate model in Section 5.1, followed by examining how the accuracy of the best surrogate model changes with different training dataset sizes in Section 5.2. Next, in Section 5.3, we assess the surrogate's performance across various locations where it hasn't been trained. Finally, Section 5.4 compares the PI accuracy when evaluated using both the surrogate and the high-fidelity EMS. For all the results shown in this section, the validation dataset was used to evaluate the accuracy of the surrogate model and the application.

5.1 Surrogate's Accuracy for Hourly Operation

The accuracy of the four models, presented in Table 5, can be found in Figure 6. The RMSE of all hourly output time series is used to compare the accuracy of all models. This RMSE provides a holistic measure of the model's accuracy. Moreover, the training and inference time were reported in Table 10.

From Figure 6, it is observed that the tuned NN outperforms the linear counterpart in terms of accuracy. This result is expected as the linear model cannot capture the inherent non-linearities of the high-fidelity model. Among the linear models,

https://doi.org/10.5194/wes-2024-96
Preprint. Discussion started: 12 August 2024

using the SVD in addition to the normalization slightly outperforms the linear model using only the normalization. However, for tuned NNs, the opposite is true. Given the broad distribution of HPP configurations, the SVD effectively captures key trends, improving the accuracy of the linear model. Yet, when tuning comes into play, the NN can make better use of all the data (in the absence of SVD) rather than a reduced representation of it (when using the SVD) which explains the difference between both tuned FNNs.

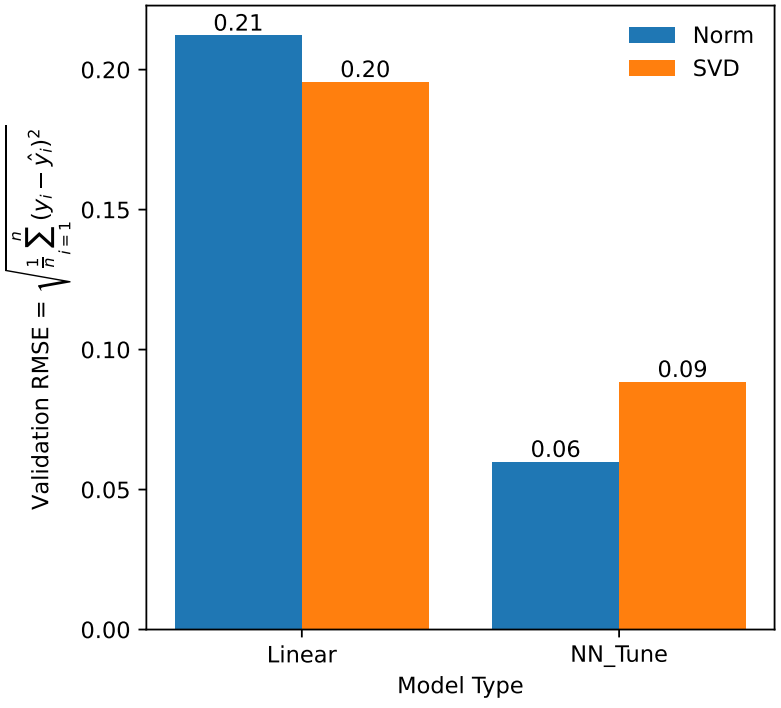

Figure 6. Validation RMSE by Data Processing Method: "Linear" for multivariate linear regression, "NN_tune" for tuned FNN (parameters in Table 7), "Norm" for Normalization only, and "SVD" for combined Normalization and SVD methods.

Table 10 contrasts the time required to execute the workflow for each surrogate model. The pre-processing time considers both training and validation datasets. However, the training time accounts only for the training dataset, while the inference time reflect the inference on a single HPP configuration spanning one year of data.

There is a substantial difference between surrogates using the normalization only and the surrogates using the SVD in addition to the normalization. This difference is even more exacerbated when looking at NN_Tuned: when using SVD the NN converges in 5 hours while it takes 7 days for the surrogate employing only a normalization. This is mainly due to the difference in training data as highlighted in Table 6.

From both presented figure and table, we conclude that the tuned FNN using the SVD provides the best compromises between accuracy, training time and execution time. To gain deeper insights into this surrogate's performance we investigated its capability to predict each hourly output time series individually, for all validation data. Figure 7 provides such an overview.

https://doi.org/10.5194/wes-2024-96
Preprint. Discussion started: 12 August 2024

eawe european academy of wind energy
Open Access WIND ENERGY SCIENCE DISCUSSIONS

Table 10. Time Metrics of Surrogate Models

Method	Model	Pre-proc.	Train Time	Inf. Time
SVD	Linear	7m	14m	0.02s
SVD	NN_Tuned	7m	5h	0.04s
Normalization	Linear	1.1m	14.4h	0.64s
Normalization	NN_Tuned	1.1m	7d	1.02s

From this figure we observed that the power output of the HPP and the curtailed power are well predicted, however the battery charge and discharge profiles are harder to predict. To further understand these discrepancies, we examine the predicted output time series for a given day, from the surrogate as well as the observed output time series from the high fidelity model.

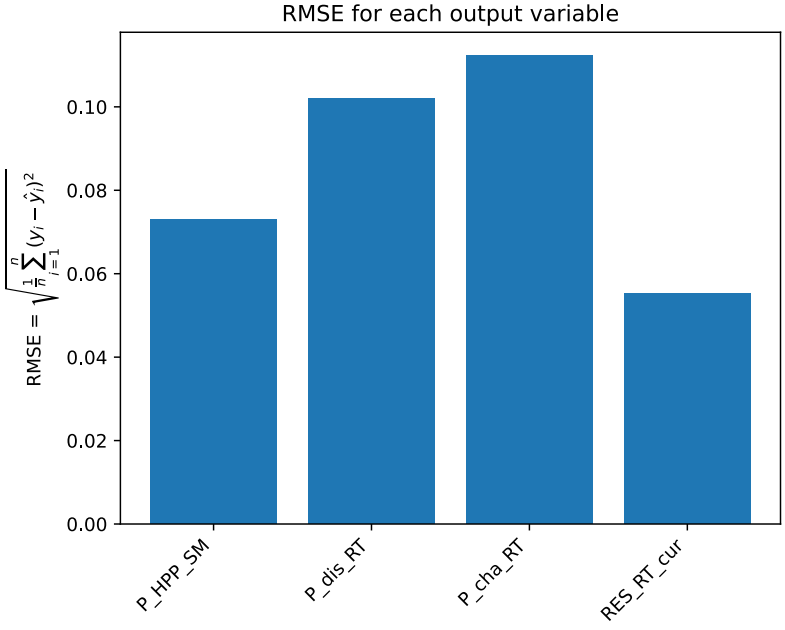

Figure 7. RMSE for each surrogate's output time series across all validation HPP configurations. P_HPP_SM is the power bidding on the SM. P_cha_RT and P_dis_RT are the charging and discharging power of the battery. RES_RT_cur is the curtailed power.

Figure 8 shows the difference between the the surrogate's prediction and the ideal behavior, from the high-fidelity model.

The surrogate captures well the daily trend across all time series. While it accurately predicts the intra-day fluctuations for power bidding, it is less precise when predicting battery charge and discharge power. This is due to the abrupt power fluctuations, in the high-fidelity model, that can be seen in Figure 8b and 8c. Additionally, as shown in Figure 8d, the surrogate occasionally struggles to forecast consistent zero values over an entire day—a challenge characteristic of FNNs. Nonetheless,

https://doi.org/10.5194/wes-2024-96
Preprint. Discussion started: 12 August 2024

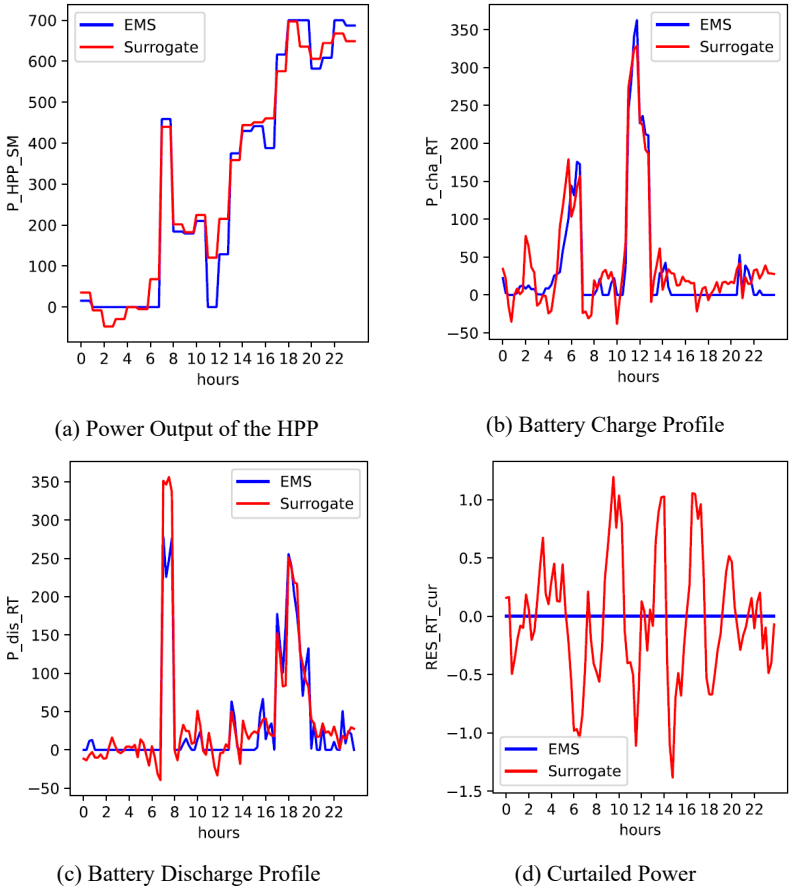

(a) Power Output of the HPP

(b) Battery Charge Profile

(c) Battery Discharge Profile

(d) Curtailed Power

Figure 8. Output time series for a given day, from the high-fidelity model (blue) and the surrogate (red). All time series are in MegaWatt.

these discrepancies are minor, with predicted curtailed power fluctuating within a ± 1.5 MW range instead of the expected steady 0 MW. Such variances are negligible relative to the HPP's export capacity, which can reach up to 700 MW.

The application presented in Section 3, requires only the HPP power output out of all the predicted output time series. That is why we want to further examine this output time series. Figure 9a presents a hexbin plot that compares hourly predicted, and normalized, HPP power outputs across all HPP configurations in the validation dataset. The hexagonal bins group nearby points and show the density of data points within each bin. The value of the density is shown on the color bar, the darker the color, the denser the hexagon. A log scale is used for clarity. A one-to-one line, representing an ideal prediction, is also depicted for comparison. The power bidding on the SM aligns closely with the observed values.

The PDF of errors, for the same data, is shown in Figure 9b. The histogram (in blue) shows the frequency distribution of these errors, while the red line represents a Gaussian (normal) distribution fitted to the data. The parameters of the Gaussian

https://doi.org/10.5194/wes-2024-96
Preprint. Discussion started: 12 August 2024

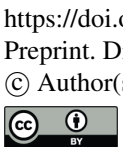

eawe european academy of wind energy
Open Access WIND ENERGY SCIENCE DISCUSSIONS

fit—mean (μ) and standard deviation (σ)—are shown in the legend and are both approximately 0.00 and 0.07, respectively. The RMSE is also 0.07, indicating the typical magnitude of prediction errors.

The mean (μ) being close to zero suggests that the surrogate's predictions are unbiased on average. The Gaussian fit's close alignment with the histogram suggests that the errors are distributed in a manner consistent with a normal distribution, which often implies that the surrogate model's residuals are well-behaved in a statistical sense.

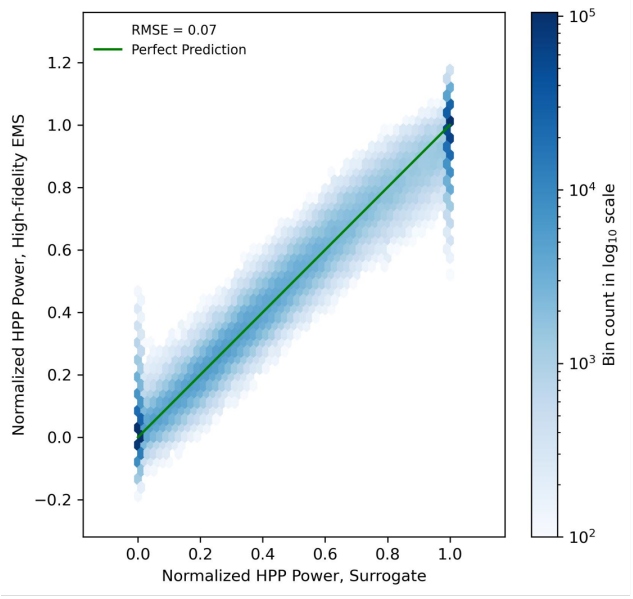

(a) Accuracy of hourly normalized Power Output for all HPP from the validation dataset predicted by the Surrogate.

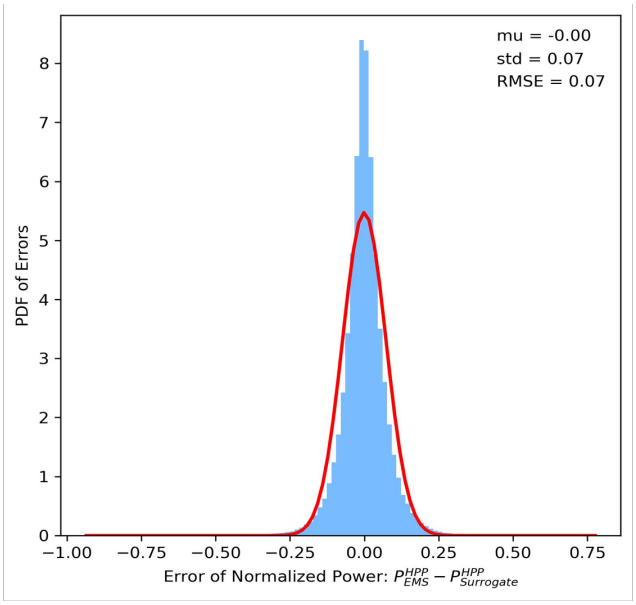

(b) PDF of error for hourly normalized Power Output for all HPP from the validation dataset predicted by the Surrogate. The red line indicates a Gaussian fit, with parameters detailed in the legend.

Figure 9. Accuracy and error distribution of hourly normalized Power Output

5.2 Surrogate Convergence to Training Dataset

The previous study has demonstrated the capacity of the NN to replicate the daily trends of the high-fidelity NN. However, the chosen data was based on an arbitrarily high number of HPP configurations. Consequently, we sought to examine how the NN's accuracy varies with different dataset sizes. NNs were tuned using the SVD processing, with a training dataset ranging from 4 to 200 HPP configurations. The validation dataset from the previous study is not modified to provide a fair comparison. Results of these simulations are illustrated in Figure 10. Interestingly, the RMSE seems to plateau when reaching a training dataset size of 110 HPP configurations. We also note that there is a marginal gain in accuracy between 50 and 100+ HPP configurations. This is relevant to highlight as it suggests potential reductions in the generated data by the high-fidelity EMS, and, therefore shorter training duration for the surrogate. As a reminder, each HPP configuration, which spans over one year of

https://doi.org/10.5194/wes-2024-96
Preprint. Discussion started: 12 August 2024

eawe european academy of wind energy
Open Access WIND ENERGY SCIENCE DISCUSSIONS

data, requires 47 minutes to generate outputs using the high-fidelity EMS. It is also interesting to compare the Normalized Root Mean Square Error (NRMSE) of yearly revenues, computed as per equation 9. The model trained with 200 HPP configurations has an NRMSE of 0.81% while the the model trained with 32 HPP configurations has an NRMSE of 1.0% across the entire validation dataset. Here again, the difference between both outcomes is marginal.

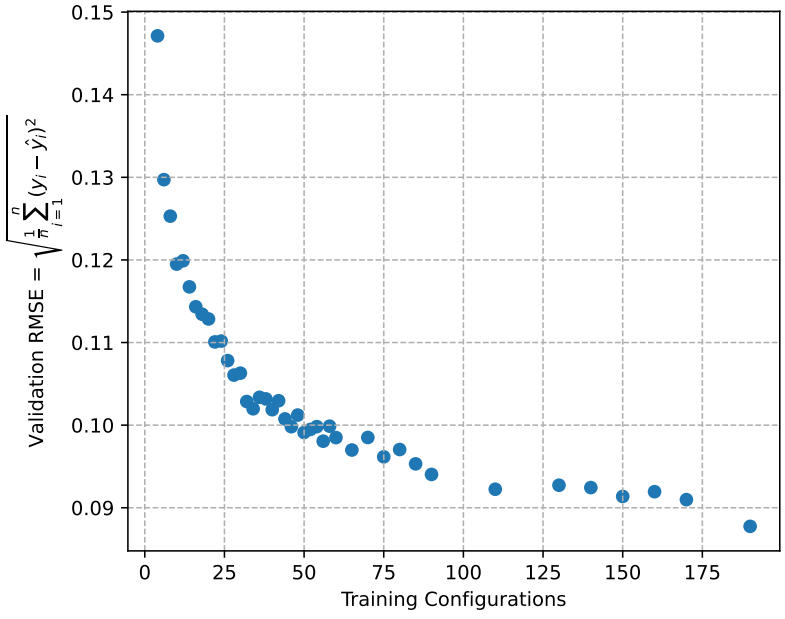

Figure 10. Evolution of accuracy with increasing training dataset size. A fixed validation dataset, of 50 configurations, is used across all simulations.

5.3 Intra-generalizability Accuracy

In the section we evaluate the surrogate's accuracy on four different locations (A to D). The selected surrogate is the tuned FNN using the SVD whose results were detailed in Section 5.1. As a reminder, this surrogate is trained using weather data from location X and with a training dataset of 200 HPP configurations. We use the NRMSE of yearly revenues to measure the accuracy of the surrogate. This was done on 10 randomly selected HPP configurations from the training dataset and 10 others from the validation dataset. All accuracy results are compared to the baseline e.g., using location X. The accuracy of the surrogate is illustrated in Figure 11.

The surrogate model's NRMSE for predicting revenue demonstrates a marginal difference between training and validation datasets. Specifically, the NRMSE for the training dataset (location X) is 0.79%, compared to 0.81% for the validation dataset. When looking at location A to D, the average NRMSE for the training dataset samples is 0.79% (aligning with the Train Baseline), whereas it is 1.3% for validation dataset samples. Notably, location D shows the greatest discrepancy in NRMSE between training and validation samples. This variation may be attributed to the combination of HPP configurations and

https://doi.org/10.5194/wes-2024-96
Preprint. Discussion started: 12 August 2024

WIND ENERGY SCIENCE DISCUSSIONS

distinct weather time series at location D, detailed in Figure 5b. Overeall, despite location X's distribution with two distinct peaks (around 0.08 and 0.1) that aren't observed in other locations, the surrogate's performance remains consistent across all locations.

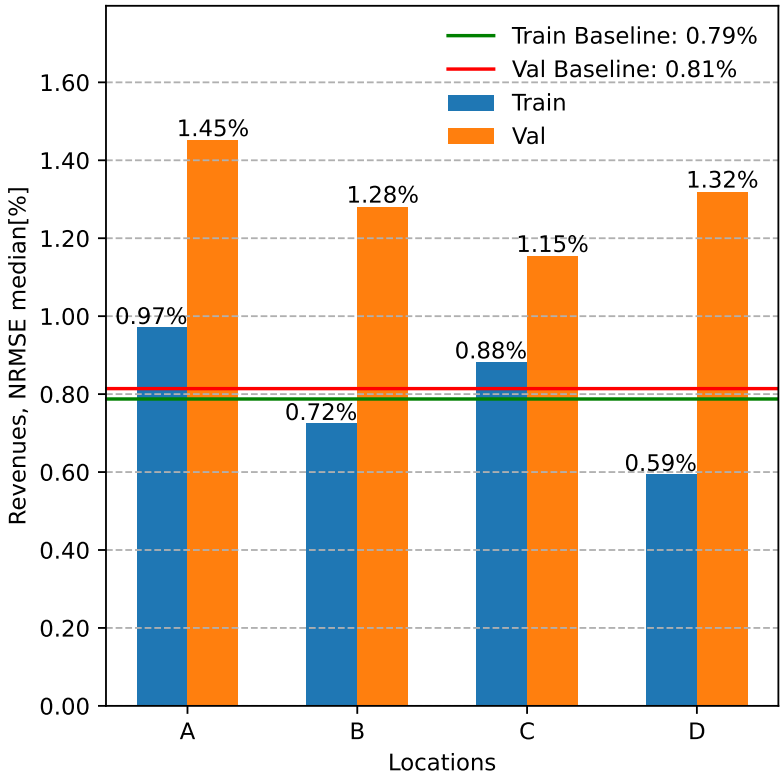

Figure 11. Performance of surrogate's generalizability for different locations and for HPP configurations from different datasets. The Baseline refers to location X, where the surrogate has been trained. Train Baseline and Val Baseline correspond to the NRMSE of Revenues from the training dataset of location X (200 HPP configurations) and from the validation dataset (50 HPP configurations). Val refers to 10 HPP configurations randomly selected from the validation dataset while Train refers to 10 random HPP configurations from the training dataset. Both Val and Train are evaluated on location A-D.

5.4 PI Evaluation Accuracy

In this section, we evaluate the PI of several HPPs using the surrogate and the high-fidelity EMS model. Both frameworks are described in Figure 3. In order to evaluate the accuracy of the PI computed with the surrogate we use the same 50 HPP configurations, from the validation dataset, for both frameworks. The selected surrogate is the tuned FNN using the SVD described in Section 5.1. Figure 12 shows the PI calculated using the high-fidelity EMS on the y-axis and the PI inferred using the surrogate on the x-axis for the corresponding HPP configuration.

https://doi.org/10.5194/wes-2024-96
Preprint. Discussion started: 12 August 2024

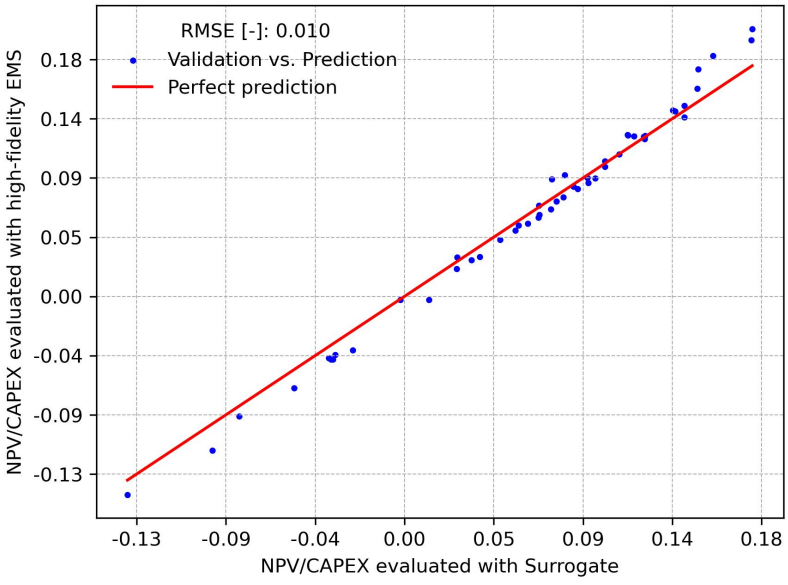

Figure 12. PI comparison based on surrogate inference and high-fidelity EMS evaluation for the validation dataset.

The RMSE of PI across the validation dataset is of 0.010, which indicates the average magnitude of the errors between the surrogate predictions and the high-fidelity EMS evaluations. The scatter plot shows that most of the points are close to the line of perfect prediction (red line), with some scatter around it. Most of the points are below the perfect line indicating that the surrogate is slightly overestimating the profitability of the HPP. However this tendency is reversed for higher NPV/CAPEX, the surrogate provides conservative estimate of the PI. Overall, the tight clustering of points around the red line suggests that the surrogate model is quite reliable for predicting the PI when compared to the high-fidelity EMS.

6 Discussion

This study aims to evaluate the potential of applying surrogate modeling in order to emulate the behavior of a complex EMS for a HPP with bidding on the spot market. Our investigation highlights the importance of both pre- and post-processing of data with an appropriate choice of the surrogate model. Among the options explored, the tuned FNN that utilizes SVD emerged as the optimal balance. Indeed, Figure 6 shows that the tuned NN using only a normalization is the most accurate, while adding an SVD results in a similar performance. Yet, when we look at the computational time, as shown in Table 10, using the SVD significantly reduces the training duration. This difference is even more pronounced when the tuning time is considered: it requires five days to tune the NN using a normalization, whereas it takes only 4.3 hours when an SVD is used. This discrepancy is assigned to the inherent capability of the SVD to extract a reduced order of data that contains meaningful coefficients and daily temporal trends.

https://doi.org/10.5194/wes-2024-96
Preprint. Discussion started: 12 August 2024

eawe european academy of wind energy
Open Access WIND ENERGY SCIENCE DISCUSSIONS

However, challenges persist, particularly in predicting battery charge and discharge profiles. As depicted in Figures 7 and 8, this difficulty arises from the high fidelity model's abrupt power output fluctuations and the intrinsic non-linearity of these variables. For the purposes of this study, focusing primarily on the power output of the HPP is sufficient, as this is the only variable required in revenue calculation and subsequent profitability index evaluation. Additionally the power output of the HPP is well predicted as shown in Figure 9b: there is no bias and the standard deviation is very small. While this result only stands for a surrogate trained with 200 HPP configurations it is still reasonable to assume similar behavior for a surrogate trained with less data points. Indeed, Figure 10 demonstrate a marginal difference in accuracy between a surrogate trained with 200 HPP configurations and 50 HPP configurations. Ultimately it is a trade off between training time and accuracy. In terms of intra-regional generalizability, the accuracy across different locations is more consistent than between dataset types. This uniformity in accuracy, within each dataset type, can be partly attributed to the region's relatively homogeneous wind profiles, facilitated by its largely flat terrain. A loss in accuracy is observed when unseen HPP configurations are used (e.g. validation dataset). Nonetheless, these results demonstrate the surrogate's ability in capturing essential data trends (Figure 11). However, it is important to note that this study's scope was confined to the DK1 market region, characterized by uniform wind profiles due to its flat terrain (Figure 5b). The fast and accurate surrogate allows us to evaluate a HPP's profitability throughout its lifetime with little computational burden. Indeed, the surrogate model is capable of evaluating the NPV/CAPEX for all 50 HPP configurations of Figure 12 in a mere 25 seconds. In contrast, computing the same evaluations using the high-fidelity model for each HPP configuration, with inputs spanning over a year, would take approximately 39 hours. However, it is important to understand the impact of the surrogate's accuracy on the the PI. Figure 12 shows that the surrogate can be reliably used if slight deviation of the order of magnitude of 0.010 PI are acceptable for the intended business evaluation. In other words, the error on the predicted NPV is around 1% of the CAPEX. It is also relevant to note that all HPP configurations are not profitable, resulting in negative PI and further supporting the use of NPV/CAPEX as an evaluation metric. Hence the importance of optimization in the context of sizing of HPP which is enabled with the developed framework. However, a detailed exploration of the sizing optimizer is beyond the scope of this manuscript and will be the subject of future investigations. It is important to emphasize that these findings are site-specific and heavily dependent on the cost model employed, hence they should not be generalized across different HPP sites.

There are certain limitations and future works worth acknowledging. For one, The full capabilities of the high-fidelity model has not been leveraged. While the EMS can consider a realisation of the forecast error in both weather and market data, our initial approach prioritized a methodology using perfect forecast data. Nonetheless, this a natural next step where a sizing framework can be developed based on a surrogate that can handle the inherent uncertainties in weather and market forecast errors.

While our research was mainly focused on the spot market, currently the major source of revenues for power plants, the market dynamics might shift. As the share of intermittent power plant increases in the grid system that is becoming more decentralized, the balancing market is forecasted to become a considerable revenue stream. Thus, there is a pressing need for a more comprehensive surrogate considering operational strategies in both spot and balancing markets.

Moreover, a FFN has it's own limitation when it comes to time series representation, as seen in the battery charge and discharge

https://doi.org/10.5194/wes-2024-96
Preprint. Discussion started: 12 August 2024

profiles on Figure 8. This highlights the importance of further exploring the machine learning field. A promising avenue would be models that blend physical constraints, such as physics-informed neural networks.

7 Conclusion

In this paper we have introduced a new methodology to accurately and efficiently approximate a state of the art EMS for HPP involved in spot market power bidding. This model leverages singular value decomposition to extract temporal trends in the input, and utilizes FNN, to represent the non-linear dynamics of the EMS. This method has demonstrated over twice the accuracy of traditional multivariate linear regression models. A key innovation of our study is the synergistic use of SVD and FFN, a combination that represents a first in this field. This approach successfully replicates the annual revenues of an HPP with an NRMSE of 0.81% for the best model. To fully demonstrate the capabilities of our surrogate model, we have integrated it into a sizing evaluation framework designed to calculate the Profitability Index (NPV/CAPEX) based on the technology mix rating within the HPP. This framework not only enabled substantial computational savings—reducing processing time from 39 hours to a mere 25 seconds compared to a high-fidelity model—but also maintained remarkable accuracy with an RMSE of 0.010. Though our methodology may seem straightforward, it is nonetheless powerful and opens up new possibilities in the field of HPP sizing optimization.

Data availability. The weather and spot market price time series data are available on request from the corresponding author.

https://doi.org/10.5194/wes-2024-96
Preprint. Discussion started: 12 August 2024

eawe european academy of wind energy
Open Access WIND ENERGY SCIENCE DISCUSSIONS

Appendix A: FNN architecture

Tables with tuned FNN architecture.

Table A1. Architecture of tuned NN using SVD

Layers	Neurons
Input Layer	17
Hidden Layer 1	80
Hidden Layer 2	60
Hidden Layer 3	80
Hidden Layer 4	80
Hidden Layer 5	80
Hidden Layer 6	80
Hidden Layer 7	60
Hidden Layer 8	80
Hidden Layer 9	80
Output Layer	125

Table A2. Place holder: Architecture of tuned NN using a normalization

Layers	Neurons
Input Layer	5
Hidden Layer 1	80
Hidden Layer 2	80
Hidden Layer 3	80
Hidden Layer 4	80
Output Layer	4

https://doi.org/10.5194/wes-2024-96
Preprint. Discussion started: 12 August 2024

eawe european academy of wind energy
Open Access WIND ENERGY SCIENCE DISCUSSIONS

Appendix B: Data supplement

Table with the coordinates of each location used in the intra-generalizability study.

Table B1. Location Coordinates for the Generalizability study. Coordinates are shown in decimal degrees.

Location	Latitude	Longitude
X	57.0482	8.8876
A	56.383	8.6705
B	55.2908	8.6551
C	57.1852	9.9527
D	55.3088	10.4398

https://doi.org/10.5194/wes-2024-96
Preprint. Discussion started: 12 August 2024

eawe european academy of wind energy
Open Access WIND ENERGY SCIENCE DISCUSSIONS

Author contributions. C.A., J.P.M.L. and K.D., conceived the research, C.A., J.P.M.L., and J.Q., developed the methodology C.A. and J.P.M.L. developed the code for the surrogate and gathered the required data, C.A., J.P.M.L., J.Q., and T.G., performed the formal analysis, J.P.M.L., K.D., S.G., and T.G. supervised the work, C.A., J.P.M.L., and J.Q., wrote the original draft and J.P.M.L., K.D., S.G., and T.G reviewed and suggested modifications for the draft.

Competing interests. The authors declare that they have no conflict of interest.

Disclaimer. This work is funded by TotalEnergies under the project "Hybrid Power Plant Life-cycle Optimization."

Acknowledgements. We would like to thank Juan-Andrés Pérez-Rúa and Poul Ejnar Sørensen for their critical feedback on the methodology and the figures as well Jenna Iori for her feedback after the first draft was written, and finally Rujie Zhu for sharing the high-fidelity EMS script.

https://doi.org/10.5194/wes-2024-96
Preprint. Discussion started: 12 August 2024

eawe european academy of wind energy
Open Access WIND ENERGY SCIENCE DISCUSSIONS

References

Abhinav, R. and Pindoriya, N. M.: Risk-constrained optimal bidding strategy for a wind power producer with battery energy storage system using extended mathematical programming, IET Renewable Power Generation, 15, 689–700, https://doi.org/https://doi.org/10.1049/rpg2.12058, 2021.

Busch, S., Kasdorp, R., Koolen, D., Mercier, A., and Spooner, M.: The Development of Renewable Energy in the Electricity Market, Tech. rep., European Commission, https://doi.org/10.2765/411281, 2023.

Cai, Z., Bussar, C., Stöcker, P., Moraes, L., Magnor, D., and Sauer, D. U.: Optimal Dispatch Scheduling of a Wind-battery-System in German Power Market, Energy Procedia, 99, 137–146, https://doi.org/https://doi.org/10.1016/j.egypro.2016.10.105, 10th International Renewable Energy Storage Conference, IRES 2016, 15-17 March 2016, Düsseldorf, Germany, 2016.

Crespo-Vazquez, J. L., Carrillo, C., Diaz-Dorado, E., Martinez-Lorenzo, J. A., and Noor-E-Alam, M.: A machine learning based stochastic optimization framework for a wind and storage power plant participating in energy pool market, Applied Energy, 232, 341–357, https://doi.org/https://doi.org/10.1016/j.apenergy.2018.09.195, 2018.

Das, K., Hansen, A. D., Koivisto, M., and Sørensen, P. E.: Enhanced features of wind-based hybrid power plants, Proceedings of the 4th International Hybrid Power Systems Workshop, 2019.

Das, K., Philippe Grapperon, A. L. T., Sørensen, P. E., and Hansen, A. D.: Optimal battery operation for revenue maximization of wind-storage hybrid power plant, Electric Power Systems Research, 189, 106 631, https://doi.org/https://doi.org/10.1016/j.epsr.2020.106631, 2020.

Dykes, K., King, J., DiOrio, N., King, R., Gevorgian, V., Corbus, D., Blair, N., Anderson, K., Stark, G., Turchi, C., et al.: Opportunities for research and development of hybrid power plants, Tech. rep., National Renewable Energy Lab.(NREL), Golden, CO (United States), 2020.

Fang, Y. and Zhao, S.: Look-ahead bidding strategy for concentrating solar power plants with wind farms, Energy, 203, 117 895, https://doi.org/https://doi.org/10.1016/j.energy.2020.117895, 2020.

Gene H. Golub, C. V. L.: Matrix computations (3rd ed.), Johns Hopkins University Press, 1996.

Huang, X., Wang, J., Huang, T., Peng, H., Song, X., and Cheng, S.: An optimal operation method of cascade hydro-PV-pumped storage generation system based on multi-objective stochastic numerical P systems, Journal of Renewable and Sustainable Energy, 13, 016 301, https://doi.org/https://doi.org/10.1063/5.0032455, 2021.

IBM: IBM® Decision Optimization Modeling for Python (DOcplex), https://github.com/IBMDecisionOptimization/docplex-doc, 2023/09/14, 2023.

Jin, R., Chen, W., and Sudjianto, A.: An efficient algorithm for constructing optimal design of computer experiments, Journal of Statistical Planning and Inference, 134, 268–287, https://doi.org/https://doi.org/10.1016/j.jspi.2004.02.014, 2005.

Kanellas, P., Das, K., Gea-Bermudez, J., and Sørensen, P.: Balancing Tool Chain: Balancing and automatic control in North Sea Countries in 2020, 2030 and 2050, DTU Wind Energy E, DTU Wind Energy, Denmark, 2020.

Kingma, D. P. and Ba, J.: ArXiv, 2017.

Koivisto, M., Das, K., Guo, F., Sørensen, P., Nuño, E., Cutululis, N., and Maule, P.: Using time series simulation tools for assessing the effects of variable renewable energy generation on power and energy systems, WIREs Energy and Environment, 8, e329, https://doi.org/https://doi.org/10.1002/wene.329, 2019.

https://doi.org/10.5194/wes-2024-96
Preprint. Discussion started: 12 August 2024

Koivisto, M., Gea-Bermúdez, J., and Sørensen, P.: North Sea offshore grid development: combined optimisation of grid and generation investments towards 2050, IET Renewable Power Generation, 14, 1259–1267, https://doi.org/https://doi.org/10.1049/iet-rpg.2019.0693, 2020a.

Koivisto, M., Jónsdóttir, G. M., Sørensen, P., Plakas, K., and Cutululis, N.: Combination of meteorological reanalysis data and stochastic simulation for modelling wind generation variability, Renewable Energy, 159, 991–999, https://doi.org/https://doi.org/10.1016/j.renene.2020.06.033, 2020b.

Li, L., Jamieson, K., DeSalvo, G., Rostamizadeh, A., and Talwalkar, A.: Hyperband: A Novel Bandit-Based Approach to Hyperparameter Optimization, Journal of Machine Learning Research, 18, 1–52, http://jmlr.org/papers/v18/16-558.html, 2018.

Lian, J., Zhang, Y., Ma, C., Yang, Y., and Chaima, E.: A review on recent sizing methodologies of hybrid renewable energy systems, Energy Conversion and Management, 199, 112 027, https://doi.org/https://doi.org/10.1016/j.enconman.2019.112027, 2019.

Lin, C., Liang, H., Pang, A., and Zhong, J.: Data-driven method of solving computationally expensive combined economic/emission dispatch problems in large-scale power systems: an improved kriging-assisted optimization approach, Frontiers in Energy Research, 11, https://doi.org/10.3389/fenrg.2023.1273760, 2023.

Long, Q., Das, K., Pombo, D. V., and Sørensen, P. E.: Hierarchical control architecture of co-located hybrid power plants, International Journal of Electrical Power & Energy Systems, 143, 108 407, https://doi.org/https://doi.org/10.1016/j.ijepes.2022.108407, 2022.

Murcia Leon, J. P., Koivisto, M. J., Sørensen, P., and Magnant, P.: Power fluctuations in high-installation-density offshore wind fleets, Wind Energy Science, 6, 461–476, https://doi.org/10.5194/wes-6-461-2021, 2021.

Pang, A., Liang, H., Lin, C., and Yao, L.: A Surrogate-Assisted Adaptive Bat Algorithm for Large-Scale Economic Dispatch, Energies, 16, https://doi.org/10.3390/en16021011, 2023.

Paska, J., Biczel, P., and Kłos, M.: Hybrid power systems – An effective way of utilising primary energy sources, Renewable Energy, 34, 2414–2421, https://doi.org/https://doi.org/10.1016/j.renene.2009.02.018, 2009.

Roy, P., He, J., Zhao, T., and Singh, Y. V.: Recent Advances of Wind-Solar Hybrid Renewable Energy Systems for Power Generation: A Review, IEEE Open Journal of the Industrial Electronics Society, 3, 81–104, https://doi.org/10.1109/OJIES.2022.3144093, 2022.

Technical University of Denmark: Sophia HPC Cluster, https://doi.org/10.57940/FAFC-6M81, 2019.

Thirunavukkarasu, M., Sawle, Y., and Lala, H.: A comprehensive review on optimization of hybrid renewable energy systems using various optimization techniques, Renewable and Sustainable Energy Reviews, 176, 113 192, https://doi.org/https://doi.org/10.1016/j.rser.2023.113192, 2023.

Wiese, F., Bramstoft, R., Koduvere, H., Pizarro Alonso, A., Balyk, O., Kirkerud, J. G., Åsa Grytli Tveten, Bolkesjø, T. F., Münster, M., and Ravn, H.: Balmorel open source energy system model, Energy Strategy Reviews, 20, 26–34, https://doi.org/https://doi.org/10.1016/j.esr.2018.01.003, 2018.

Xu, B., Oudalov, A., Ulbig, A., Andersson, G., and Kirschen, D. S.: Modeling of Lithium-Ion Battery Degradation for Cell Life Assessment, IEEE Transactions on Smart Grid, 9, 1131–1140, https://doi.org/10.1109/TSG.2016.2578950, 2018.

Zhang, G., Hu, W., Cao, D., Liu, W., Huang, R., Huang, Q., Chen, Z., and Blaabjerg, F.: Data-driven optimal energy management for a wind-solar-diesel-battery-reverse osmosis hybrid energy system using a deep reinforcement learning approach, Energy Conversion and Management, 227, 113 608, https://doi.org/https://doi.org/10.1016/j.enconman.2020.113608, 2021.

Zhu, L.-P., Yin, X., and Zhu, L.-X.: Dimension Reduction via an Alternating Inverse Regression, Journal of Computational and Graphical Statistics, http://www.jstor.org/stable/25765379, 2010.

https://doi.org/10.5194/wes-2024-96
Preprint. Discussion started: 12 August 2024

eawe european academy of wind energy
Open Access WIND ENERGY SCIENCE DISCUSSIONS

Zhu, R., Das, K., Sørensen, P. E., and Hansen, A. D.: Optimal Participation of Co-located Wind-battery Plants in Sequential Electricity Markets, TechRxiv. Preprint, https://doi.org/10.36227/techrxiv.21618984.v1, 2022.